

# A stability analysis of radiative shocks in the presence of a transverse magnetic field

Babulakshmanan Ramachandran<sup>★</sup> and Michael D. Smith<sup>★</sup>

*Armagh Observatory, College Hill, Armagh BT61 9DG*

Accepted 2005 July 5. Received 2005 July 3; in original form 2005 April 1

## ABSTRACT

Radiative shock waves may be subject to a global thermal instability in which the cooling layer and shock front undergo growing resonant oscillations. For strong hydrodynamic shocks, the presence of the overstability depends on the temperature and density indices of power-law cooling functions and the specific heat ratio ( $\alpha$ ,  $\beta$  and  $\gamma$ , respectively). Here, we investigate the stabilizing influence of a transverse magnetic field by introducing the shock Alfvén number,  $M_a$ , as a fourth parameter. We thus investigate the stability criteria for both molecular and atomic shocks under a wide range of conditions. In particular, we find that all molecular shocks in which the cooling increases with the temperature ( $\alpha > 0$ ) are stabilized to the first four modes if  $M_a < 20$  ( $\beta = 2$ ). For  $\alpha = -0.5$ , the first overtone remains stable only for  $M_a < 8$ . We conclude that molecular shocks in the interstellar medium are probably stabilized by a transverse magnetic field unless exceptional circumstances arise in which the cooling strongly increases as the gas cools.

**Key words:** instabilities – magnetic fields – MHD – shock waves – ISM: molecules.

## 1 INTRODUCTION

To interpret observations of an astrophysical shock, we need to know if it can be compared to steady-state models or if it is subject to an instability. In fact, the cooling immediately downstream of a shock front may lead to an overstability of the entire radiative shock wave (Langer, Chanmugam & Shaviv 1981). For hydrodynamic flows, a linear analysis yields conditions for growing oscillations as well as their particular frequencies (Chevalier & Imamura 1982), and many analytical and numerical studies have been presented, as recently summarized by Ramachandran & Smith (2005, hereafter Paper 1). However, the growth of the oscillations will be damped by a magnetic field. A transverse field not only reduces the immediate post-shock temperature and compression but could also completely stabilize the cooling layer. The first question is: How strong does the field have to be to ensure stability? This question has been answered for the important case of fast shocks into atomic gas (Toth & Draine 1993; Kimoto & Chernoff 1997). Here, we extend these results to include power-law cooling functions pertaining to other interstellar conditions: a molecular gas and a medium in which the energy levels relevant to the cooling are maintained in local thermodynamic equilibrium. The conclusions take on added significance through the latest campaigns to explore infrared and submillimetre regimes with spectroscopic methods (e.g. with *Spitzer* and *Herschel*).

A linear analysis of plane-parallel radiative shocks with a transverse field was performed by Toth & Draine (1993). They assumed a specific heat ratio  $\gamma$  of  $5/3$  and a cooling function  $\Lambda \propto \rho^2 T^\alpha$ , where  $\rho$  is the density and  $T$  is the temperature. Only the index  $\alpha$  determines the stability in the absence of a magnetic field provided the shock is strong. The latter assumption eliminates the Mach number,  $M$ , from the problem. Here,  $M = u_{in}/c_s$  where  $u_{in}$  is the shock speed and  $c_s$  is the upstream sound speed.

On the other hand, the Alfvén number  $M_a = u_{in}/v_a$ , where  $v_a$  is the upstream Alfvén speed, is a second variable when a significant magnetic field is present. Toth & Draine (1993, hereafter TD93) found, as an example, that even a quite weak field ( $M_a < 8$ ) will suppress the growth of all modes of oscillation for  $\alpha > 0$ . For  $\alpha = 0.5$ , even weaker fields ( $M_a < 33$ ) are enough to stabilize a shock. Their numerical study agreed with the linear analysis and also revealed that, for shock speeds  $v_s < 160 \text{ km s}^{-1}$ , radiative shocks occurring in interstellar gas with  $n_H \leq 0.4 \text{ cm}^{-3}$  may be magnetically stabilized. Further simulations by Kimoto & Chernoff (1997), however, also demonstrated that the typical interstellar field may not be sufficient to stabilize shocks if  $\alpha < 0$ . The fundamental mode can generate very large-amplitude oscillations. Moreover, even when the fundamental is stabilized, the overtones can still produce higher-frequency oscillations of substantial amplitude.

The general linear analysis for hydrodynamic flows was extended in Paper 1 to include molecular shocks. The dependence on three parameters,  $\alpha$ ,  $\beta$  and  $\gamma$ , was considered, where  $\beta$  is the density dependence of the cooling

$$\Lambda \propto \rho^\beta T^\alpha. \quad (1)$$

<sup>★</sup>E-mail: brc@arm.ac.uk (BR); mds@arm.ac.uk (MDS)

A strong dependence on  $\gamma$  was found, with the regime of over-stability significantly reduced for molecular shocks. In particular, the fundamental mode grows only for  $\alpha < -0.24$  in the molecular equivalent ( $\gamma = 7/5$  and  $\beta = 2$ ) of the atomic case (for which  $\alpha < 0.38$  is required). However, the overtones are more significant in molecular shocks with, for example, the first overtone growing for  $\alpha < 0.66$ . Building on this work, we introduce the Alfvén number here as the fourth parameter, to determine the influence of the magnetic field.

In the molecular shocks discussed here, we presume that the fraction of mass in ions is sufficiently high that ion-magnetosonic waves cannot propagate ahead of the shock front. Otherwise, if the fraction of ions were low, the magnetic field would drift through the neutral molecules, a process termed ‘ambipolar diffusion’. Friction between the ions and neutrals may then replace the molecular viscosity, changing the nature of the shock front. We discuss this restriction in Section 3. Other dynamic instabilities are then possible in such continuous shocks (as well as in jump shocks, see Paper 1 for a summary). The jump shocks studied here thus require a source of ionization that does not cause wholesale molecular dissociation. This may occur near the edges of molecular clouds partially exposed to the ultraviolet from nearby OB associations, as proposed for the HH 90/91 shock (Smith 1994b). The ions can be dust grains, molecules or atoms, according to the physical conditions.

In this paper, we extend the formalism of TD93. Starting with the steady-state radiative shock structure, we perturb the shock velocity and determine the growth or damping rate in addition to the oscillatory period. We study the one-dimensional case while ignoring thermal conduction as well as radiation transfer. In the hydrodynamic case, a stationary wall of infinite density is assumed to lie downstream of the shock front. In the magnetohydrodynamic (MHD) analysis, the density in the downstream gas rises towards a finite constant value. In order to make the problem tractable, we ensure not only that the temperature continues to fall, reaching zero kelvin, but also that the temperature perturbation also vanishes at the downstream boundary. Then, waves escaping downstream are constrained to be pure Alfvén waves, leading to a straightforward boundary condition. In this respect, it should be noted that the published versions of equation (A27) of TD93 (where the minus sign should be replaced by a plus sign) and equation (2) of Kimoto & Chernoff (1997) (where the conditionals should be reversed) are incorrect.

In Paper 1, we undertook a linear stability analysis similar to Imamura et al. (1996) while taking a general  $\gamma$  so as to encompass molecular shocks. By also generalizing the density index, we take into account different physical situations. In particular,  $\beta = 1$  corresponds to cases where the energy levels of the atoms or molecules that provide the dominant cooling are in local thermodynamic equilibrium. For example, this can correspond to  $\text{H}_2$  cooling in warm gas for densities above  $\sim 10^4 \text{ cm}^{-3}$  provided hydrogen atoms act as the main collision partner. The specific heat ratio  $\gamma = 5/3$  remains appropriate for dissociative shocks. The value  $\gamma = 7/5$  applies to a pure  $\text{H}_2$  gas while, more realistically for the interstellar medium,  $\gamma = 10/7$  accounts for the addition of 10 per cent helium atoms.

## 2 FORMULATION OF THE PROBLEM

### 2.1 The equations

We consider a reference frame in which an ambient gas of uniform density  $\rho_a$  and supersonic speed  $u_{in}$  passes through a stationary shock front at  $x = x_s$  from upstream, i.e. to the right in Fig. 1, as

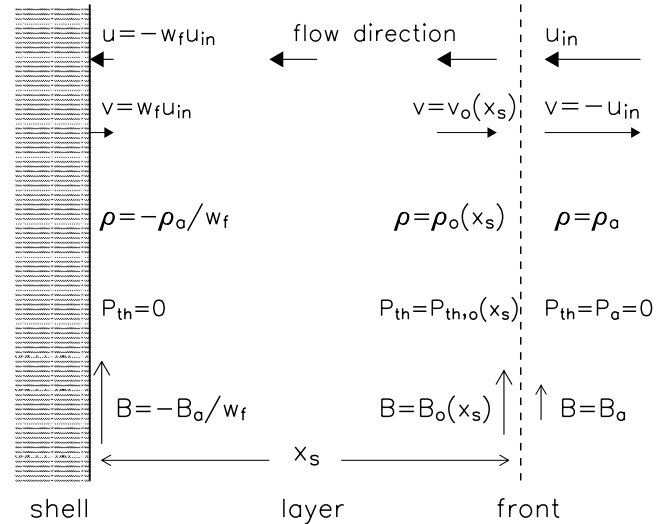


**Figure 1.** A sketch of the steady shock configuration. The shock jump conditions are defined by equations (16), (17) and (18); the total compression,  $-w_f$ , is given by equation (22). Note that, under strong shock conditions, the upstream thermal pressure is equated to zero.

defined by Chevalier & Imamura (1982). The gas cools and collapses before reaching a cold shell at  $x = 0$ , also of uniform density. The approach speed  $u_{in}$  is defined as a positive quantity. Therefore, the pre-shock gas velocity is  $v = -u_{in}$ . In this frame, the material in the shell is moving downstream, thus making space for the accumulation of new material.

Following TD93, we take a perpendicular magnetic field,  $B_a$ , which is frozen in to the gas and so increases in proportion to the density. The shock Alfvén (Mach) number is defined as  $M_a = u_{in}/v_a$  where  $v_a$  is the Alfvén speed in the ambient medium. The magnetic pressure in the flow is then

$$P_B = b\rho^2, \quad (2)$$

where the constant  $b$  is

$$b = \frac{B_a^2}{8\pi\rho_a^2} = \frac{v_a^2}{2}, \quad (3)$$

and we define the useful parameter  $\theta$  (the parameter  $\beta$  of TD93) as

$$\theta = \frac{B_a^2}{8\pi\rho_a u_{in}^2} = \frac{1}{2M_a^2}, \quad (4)$$

which is the ratio of the magnetic pressure to the upstream ram pressure.

The one-dimensional hydrodynamical equations are (e.g. TD93)

$$\frac{\partial\rho}{\partial t} + \frac{\partial(\rho v)}{\partial x} = 0, \quad (5)$$

$$\rho \left( \frac{\partial v}{\partial t} + v \frac{\partial v}{\partial x} \right) + \frac{\partial P}{\partial x} = 0 \quad (6)$$

and

$$\frac{\partial e}{\partial t} + \frac{\partial(ev)}{\partial x} = -\frac{\partial(Pv)}{\partial x} - \Lambda, \quad (7)$$

where  $\Lambda$  is the radiated energy loss per unit volume and  $P$  is the total (magnetic plus thermal) pressure, related to the internal energy by

$$e = \frac{P}{\gamma - 1} + \left( 1 - \frac{1}{\gamma - 1} \right) \frac{B^2}{8\pi} + \frac{1}{2}\rho v^2. \quad (8)$$

Equations (5), (6) and (7) refer to the conservation of mass, momentum and energy, respectively. Eliminating  $e$ ,

$$\frac{\partial P}{\partial t} + v \frac{\partial P}{\partial x} + [\gamma P + b\rho^2(2 - \gamma)] \frac{\partial v}{\partial x} = -(\gamma - 1)A\rho^{\beta-\alpha}(P - b\rho^2)^\alpha, \quad (9)$$

where  $A$  is a constant and we have used the ideal gas law to eliminate temperature.

## 2.2 The steady state

The steady-state solution is denoted by the subscript 0. Equations (5) and (6) are integrated to yield

$$\rho_0 v_0 = -\rho_a u_{\text{in}} \quad (10)$$

and

$$P_0 = \rho_a u_{\text{in}}(v_0 + u_{\text{in}}) + b\rho_a^2. \quad (11)$$

Equations (10) and (11) are substituted in equation (9), which results in

$$\frac{dv_0}{dx} = \frac{C(-\rho_a u_{\text{in}})^{\beta-1} [-v_0^2 - u_{\text{in}}v_0 + \rho_a b (\frac{u_{\text{in}}}{v_0} - \frac{v_0}{u_{\text{in}}})]}{v_0^\beta [v_0 + \gamma(v_0 + u_{\text{in}}) + \rho_a b (\frac{\gamma}{u_{\text{in}}} + \frac{u_{\text{in}}(2-\gamma)}{v_0^2})]}, \quad (12)$$

where

$$C = (\gamma - 1)A.$$

This equation can be integrated to determine the velocity through the shocked layer. We now introduce the following variables:

$$\xi = \frac{x}{x_s}, \quad (13)$$

$$w = \frac{v_0}{u_{\text{in}}}. \quad (14)$$

Equations (12), (13) and (14) lead to

$$\frac{d\xi}{dw} = \frac{-(-w)^\beta [w + \gamma(1 + w + \theta) + \frac{(2-\gamma)\theta}{w^2}]}{u_{\text{in}}^{2\alpha-3} C \rho_a^{\beta-1} x_s (-w - w^2 - \theta w + \frac{\theta}{w})^\alpha}. \quad (15)$$

The jump condition across the steady shock front can be written as (Smith 1989)

$$\rho_0(x_s) = \rho_a q, \quad (16)$$

$$v_0(x_s) = -\frac{u_{\text{in}}}{q}, \quad (17)$$

$$P_0(x_s) = \rho_a u_{\text{in}}^2 \left(1 - \frac{1}{q} + \theta\right), \quad (18)$$

where the shock front compression is

$$q = \frac{(U + V)}{4\theta(2 - \gamma)},$$

$$U = -(\gamma - 1 + 2\gamma\theta),$$

$$V = \sqrt{4\gamma\theta[\gamma\theta - (\gamma - 1)] + (\gamma - 1)^2 + 16\theta}. \quad (19)$$

The boundary condition at  $x = 0$  is determined from the fact that the temperature is zero, the total pressure is equal to the magnetic pressure and the density remains finite:

$$P_0(x = 0) = P_B(x = 0). \quad (20)$$

If we denote the velocity of the shell as  $v_0(x = 0)$ , and also define  $w_f = v_0(x = 0)/u_{\text{in}}$ , from (2) and (11) we can then write the expression

$$\rho_a u_{\text{in}}^2(1 + w_f + \theta) = \rho_a u_{\text{in}}^2(\theta/w_f^2). \quad (21)$$

The physical solution to the above cubic equation is

$$w_f = \frac{-\theta - \sqrt{(\theta^2 + 4\theta)}}{2}. \quad (22)$$

Note that  $-1/w_f$  is the total compression, as indicated in Fig. 1.

## 2.3 The set of linear equations

The shock wave is now perturbed by

$$\frac{dx_s}{dt} = v_{s1} e^{\sigma t}, \quad (23)$$

where  $\sigma = \sigma_R + i\sigma_I$  is the frequency and  $v_{s1}$  is a real quantity. The position of the shock may be represented as the real part of

$$x_s = x_{s0} + x_{s1} e^{\sigma t}, \quad (24)$$

where  $x_{s1} = v_{s1}/\sigma$ . Considering only the terms up to first order:

$$\xi = \frac{x}{x_s} = \frac{x}{x_{s0}} \left(1 - \frac{x_{s1}}{x_{s0}} e^{\sigma t}\right), \quad (25)$$

$$\frac{\partial \xi}{\partial x} = \frac{1}{x_{s0}} \left(1 - \frac{x_{s1}}{x_{s0}} e^{\sigma t}\right), \quad (26)$$

$$\frac{\partial \xi}{\partial t} = -\frac{x x_{s1} \sigma e^{\sigma t}}{x_{s0}^2}, \quad (27)$$

$$\rho = \rho_0(\xi) + \rho_1(\xi) e^{\sigma t}, \quad (28)$$

$$P = P_0(\xi) + P_1(\xi) e^{\sigma t}, \quad (29)$$

$$v = v_0(\xi) + v_1(\xi) e^{\sigma t}. \quad (30)$$

All the quantities with subscript 1 represent the small perturbed factors.

When the shock is moving, we consider the frame of reference in which the shock is stationary, i.e. the upstream velocity is now  $-u_{\text{in}} - v_{s1} e^{\sigma t}$ . The boundary conditions at the moving shock wave are obtained by taking the derivatives of equations (16), (17) and (18) with respect to  $u_{\text{in}}$  to obtain

$$\rho_1(x = x_s) = 2v_{s1}\theta q^2 \frac{\rho_a}{u_{\text{in}}} \frac{d(1/q)}{d\theta}, \quad (31)$$

$$P_1(x = x_s) = 2v_{s1}\rho_a u_{\text{in}} \left[1 - \frac{1}{q} + \theta \frac{d(1/q)}{d\theta}\right], \quad (32)$$

$$v_1(x = x_s) = v_{s1} \left[2\theta \frac{d(1/q)}{d\theta} - \frac{1}{q}\right] + v_{s1}, \quad (33)$$

where the last term in (33) arises because of the transformation of coordinates to the shock frame.

We will also need the derivative of  $q$ , which is, from equation (19),

$$\frac{d(1/q)}{d\theta} = \left\{ \gamma + \frac{4 + \gamma[2\gamma\theta - (\gamma - 1)]}{\sqrt{V}} \right\} \times \left[ \frac{2 - \gamma}{2 - \gamma(\gamma - 1)} \right]. \quad (34)$$

We then transform to the following variables:

$$\zeta = \frac{x_{s0}\sigma\rho_1}{v_{s1}\rho_a}, \quad (35)$$

$$\pi = \frac{P_1}{v_{s1}\rho_a u_{in}}, \quad (36)$$

$$\eta = \frac{v_1}{v_{s1}}, \quad (37)$$

$$\delta = \frac{x_{s0}\sigma}{u_{in}}. \quad (38)$$

At the shock front, from (31)–(33), the new variables take the following values:

$$\xi(w = w_s) = 1, \quad (39)$$

$$\zeta(w = w_s) = 2\delta\theta q^2 \frac{d(1/q)}{d\theta}, \quad (40)$$

$$\pi(w = w_s) = 2 \left[ 1 - \frac{1}{q} + \theta \frac{d(1/q)}{d\theta} \right], \quad (41)$$

$$\eta(w = w_s) = \left[ 2\theta \frac{d(1/q)}{d\theta} - \frac{1}{q} + 1 \right]. \quad (42)$$

Substituting (28), (29) and (30) into (5), (6) and (9), the fluid equations can be rewritten as

$$-\frac{\xi}{w^2} + \zeta \frac{d\xi}{dw} + \frac{w}{\delta} \frac{d\zeta}{dw} + \frac{\eta}{w^2} - \frac{1}{w} \frac{d\eta}{dw} + \frac{\zeta}{\delta} = 0, \quad (43)$$

$$-\xi + \delta \frac{d\xi}{dw} \eta + w \frac{d\eta}{dw} + \eta - \frac{w^2}{\delta} \zeta - w \frac{d\pi}{dw} = 0, \quad (44)$$

$$D + E = F, \quad (45)$$

where

$$D = \left( -\xi + \delta \frac{d\xi}{dw} \pi + w \frac{d\pi}{dw} + \eta - \frac{w}{\delta} + \pi\gamma \right),$$

$$E = \left( -\frac{\xi}{w^2} + \zeta \frac{d\xi}{dw} + \frac{w}{\delta} \frac{d\zeta}{dw} + \frac{\eta}{w^2} - \frac{1}{\delta w} + \frac{\zeta}{\delta} \right)$$

$$\times \left[ \gamma(w + 1 + \theta) + \frac{(2 - \gamma)\theta}{w^2} \right] w - \frac{2(2 - \gamma)\xi\theta}{w\delta},$$

$$F = \left[ w + \gamma(1 + w + \theta) + \frac{(2 - \gamma)\theta}{w^2} \right]$$

$$\times \left[ \alpha\pi - (\beta - \alpha)(1 + w + \theta) \frac{\zeta w}{\delta} + (\beta + \alpha) \frac{\zeta\theta}{\delta w} \right]$$

$$\times \left( w + 1 + \theta - \frac{\theta}{w^2} \right)^{-1}.$$

The quantities  $\zeta$ ,  $\pi$  and  $\eta$  are complex eigenfunctions. We will employ the subscripts ‘r’ and ‘i’ to denote the real and imaginary components of the above quantities. The quantity  $\delta$  is a complex number with the sign of the real part,  $\delta_r$ , indicating the instability (positive value) or stability (negative value) of a mode. The quantity  $\delta_i$  is interpreted as the eigenfrequency, in units of  $(u_{in}/x_{s0})$ . The equations for the real and complex quantities are provided in Appendix A.

## 2.4 The integration process

While integrating the above equations, we find that there are numerical problems when  $\alpha \leq 0.2$  as the temperature approaches zero. To solve this, we follow a prescription suggested by TD93, which is to introduce a break in the power-law cooling at a temperature  $T_c$ , at a velocity  $w_c$ , leaving a small region near the shell where the cooling function will have  $\alpha = 0.5$ . Therefore, the cooling function is split into two regimes such that

$$\Lambda = A\rho^{\beta-\alpha}(P - b\rho^2)^\alpha \quad \text{at } w < w_c, \quad (46)$$

$$\Lambda = A_c\rho^{\beta-\alpha_c}(P - b\rho^2)^{\alpha_c} \quad \text{at } w > w_c. \quad (47)$$

Here,  $A_c = A(P_c - b\rho_c^2)^{\alpha-\alpha_c}$  and  $(P_c - b\rho_c^2)/\rho_c \equiv 0.001u_{in}^2$ , as in TD93. To obtain the shock length, we integrate equation (15) from  $\xi = 1$  to  $\xi = 0$  and take into account the two-component cooling function.

The boundary condition at the shell for a moving shock under the influence of a transverse magnetic field is derived in Appendix B. It is more complicated than in Paper 1, where the gas settles on the wall. In the present scenario, the velocity of the gas does not vanish since the magnetic pressure limits the compression. The boundary condition is

$$\left| \pi \sqrt{-w^3/(2\beta)} + \eta \right| = 0, \quad (48)$$

similar to TD93 but correcting a typographical error in their equation (A27).

For the various combinations of the four free parameters,  $\alpha$ ,  $\beta$ ,  $\gamma$  and  $\theta$ , the quantities  $\delta_r$  and  $\delta_i$  are determined by imposing the boundary condition at the shell boundary. We solved the differential equations employing a fourth-order Runge–Kutta technique for trial values of  $\delta_r$  and  $\delta_i$  selected from a grid of points uniformly covering the complex plane. The combinations that come closest to satisfying the boundary condition for each mode determine a new set of grid points with a higher resolution.

## 3 GENERAL RESULTS

We have calculated the growth rates ( $\delta_r$ ) and eigenfrequencies ( $\delta_i$ ) for the various cases of  $\alpha$ ,  $\beta$  and  $\gamma$  with weak ( $M_a = 30$ ), intermediate ( $M_a = 10$ ) and strong ( $M_a = 3$ ) magnetic fields for the fundamental mode as well as the first three overtones. These results are presented in Tables 1–8. Equivalent tables for the case  $\gamma = 10/7$  have been constructed but are not presented here. We plot the growth rates against  $\alpha$  in Fig. 2 for various modes. The major results are as follows.

(i) We have accurately reproduced the results of TD93 for the specific case  $\beta = 2$  and  $\gamma = 5/3$  (Tables 2 and 6) as a specific case in our parametric space.

(ii) The fact that the instability regime becomes increasingly restricted with an increase in the transverse magnetic field holds for all values of  $\alpha$ ,  $\beta$  and  $\gamma$ .

(iii) The fundamental remains the most restricted mode to be unstable. The field has a similar stabilizing effect on all the modes.

(iv) The lower value for the density index  $\beta$  provides more stability. However, for high magnetic fields (solid lines in Fig. 2), the stability criterion becomes independent of  $\beta$ . This is interpreted as the cushion effect of the field which limits the compression.

(v) With decreasing  $\gamma$ , the instability regime is more restricted for all magnetic field strengths. Whether the molecular gas is diatomic ( $\gamma = 7/5$ ) or contains helium ( $\gamma = 10/7$ ) does not significantly alter the instability regime.

**Table 1.** Growth rates ( $\delta_r$ ) for several modes and magnetic field strengths, as measured by the Alfvén number  $M_a$ , for  $\gamma = 5/3$  and  $\beta = 1$ .

$\alpha$	Fundamental			First overtone		
	$M_a = 3$	$M_a = 10$	$M_a = 30$	$M_a = 3$	$M_a = 10$	$M_a = 30$
-1	-0.02942	0.04903	0.08965	0.06387	0.11420	0.14986
-0.5	-0.08446	0.00567	0.03646	-0.03742	0.03890	0.07482
0.0	-0.18538	-0.05842	-0.02296	-0.20521	-0.06762	-0.01974
0.3	-0.29720	-0.11769	-0.07122	-0.38342	-0.16282	-0.09245
0.5	-0.42465	-0.17862	-0.11462	-0.57743	-0.25705	-0.15414
$\alpha$	Second overtone			Third overtone		
	$M_a = 3$	$M_a = 10$	$M_a = 30$	$M_a = 3$	$M_a = 10$	$M_a = 30$
-1	0.11050	0.13937	0.16695	0.13817	0.16075	0.19142
-0.5	-0.00862	0.04990	0.07818	0.00809	0.06541	0.09936
0.0	-0.20728	-0.07856	-0.03713	-0.21087	-0.07366	-0.02433
0.3	-0.42137	-0.19620	-0.12957	-0.45058	-0.20419	-0.12893
0.5	-0.65377	-0.31342	-0.21165	-0.70913	-0.33717	-0.22760

**Table 2.** Growth rates ( $\delta_r$ ) for several modes and magnetic field strengths for  $\gamma = 5/3$  and  $\beta = 2$ . This table can be compared to table 1 of TD93.

$\alpha$	Fundamental			First overtone		
	$M_a = 3$	$M_a = 10$	$M_a = 30$	$M_a = 3$	$M_a = 10$	$M_a = 30$
-1	-0.03549	0.04610	0.09351	0.06696	0.13981	0.19781
-0.5	-0.08877	0.01342	0.04383	-0.02921	0.08413	0.13291
0.0	-0.17983	-0.02853	0.00702	-0.18560	0.00496	0.06983
0.3	-0.27889	-0.06263	-0.01806	-0.35272	-0.06229	0.02479
0.5	-0.39054	-0.09283	-0.03697	-0.53889	-0.12623	-0.00998
$\alpha$	Second overtone			Third overtone		
	$M_a = 3$	$M_a = 10$	$M_a = 30$	$M_a = 3$	$M_a = 10$	$M_a = 30$
-1	0.11374	0.17466	0.22738	0.14253	0.19826	0.25109
-0.5	0.00067	0.10719	0.16104	0.01897	0.12425	0.18399
0.0	-0.18654	0.00890	0.08662	-0.18846	0.01377	0.10306
0.3	-0.38992	-0.08046	0.03131	-0.41714	-0.09122	0.04081
0.5	-0.61605	-0.17289	-0.01352	-0.67020	-0.20545	-0.01179

**Table 3.** Growth rates ( $\delta_r$ ) for several modes and magnetic field strengths for  $\gamma = 7/5$  and  $\beta = 1$ .

$\alpha$	Fundamental			First overtone		
	$M_a = 3$	$M_a = 10$	$M_a = 30$	$M_a = 3$	$M_a = 10$	$M_a = 30$
-1	-0.12574	-0.03009	0.00029	-0.04055	0.02876	0.06090
-0.5	-0.18312	-0.06286	-0.02743	-0.13786	-0.02838	0.01337
0.0	-0.28865	-0.11479	-0.06609	-0.30446	-0.11369	-0.05206
0.3	-0.40691	-0.16801	-0.10022	-0.48460	-0.19620	-0.10778
0.5	-0.53663	-0.22589	-0.13324	-0.67452	-0.28096	-0.16065
$\alpha$	Second overtone			Third overtone		
	$M_a = 3$	$M_a = 10$	$M_a = 30$	$M_a = 3$	$M_a = 10$	$M_a = 30$
-1	0.00362	0.04071	0.05939	0.02880	0.06460	0.08899
-0.5	-0.11048	-0.02764	0.00114	-0.09556	-0.09275	0.02439
0.0	-0.30800	-0.13002	-0.07824	-0.31358	-0.12335	-0.06976
0.3	-0.52493	-0.22824	-0.14361	-0.55789	-0.23731	-0.15350
0.5	-0.74988	-0.32688	-0.20005	-0.80390	-0.35412	-0.22737

(vi) The frequency of the fundamental decreases strongly as  $\alpha$  decreases for all magnetic field strengths. The frequency of the overtones generally tends to a constant value as  $\alpha$  decreases. Note that in Fig. 3 the frequencies of the modes have been normalized by a

factor of  $2n + 1$ , where  $n$  is the mode number, for display purposes and so demonstrates that, for all magnetic field strengths, the resonant frequencies are analogous to the acoustic modes in a half-open organ pipe.

**Table 4.** Growth rates ( $\delta_r$ ) for several modes and magnetic field strengths for  $\gamma = 7/5$  and  $\beta = 2$ .

$\alpha$	Fundamental			First overtone		
	$M_a = 3$	$M_a = 10$	$M_a = 30$	$M_a = 3$	$M_a = 10$	$M_a = 30$
-1	-0.12850	-0.02761	0.01627	-0.03781	0.04672	0.08856
-0.5	-0.18572	-0.04914	-0.01205	-0.13274	0.00162	0.05346
0.0	-0.28557	-0.08540	-0.03462	-0.29240	-0.06666	0.01054
0.3	-0.39682	-0.11950	-0.05177	-0.46628	-0.13231	-0.02255
0.5	-0.51900	-0.15418	-0.06567	-0.65304	-0.20231	-0.05032

$\alpha$	Second overtone			Third overtone		
	$M_a = 3$	$M_a = 10$	$M_a = 30$	$M_a = 3$	$M_a = 10$	$M_a = 30$
-1	0.00628	0.06857	0.10574	0.03269	0.09028	0.13057
-0.5	-0.10479	0.01285	0.06522	-0.08846	0.02882	0.08690
0.0	-0.29458	-0.07317	0.01163	-0.29851	-0.06802	0.02653
0.3	-0.50449	-0.15932	-0.03224	-0.53521	-0.16798	-0.02552
0.5	-0.72683	-0.25388	-0.07193	-0.77992	-0.27967	-0.07602

**Table 5.** Eigenfrequencies ( $\delta_i$ ) for several modes and magnetic field strengths for  $\gamma = 5/3$  and  $\beta = 1$ .

$\alpha$	Fundamental			First overtone		
	$M_a = 3$	$M_a = 10$	$M_a = 30$	$M_a = 3$	$M_a = 10$	$M_a = 30$
-1	0.44847	0.33935	0.30432	1.45520	1.03328	0.92059
-0.5	0.50430	0.37630	0.34126	1.50546	1.03500	0.91030
0.0	0.58627	0.41387	0.36464	1.59283	1.03047	0.87269
0.3	0.67073	0.44723	0.37841	1.68773	1.02950	0.83627
0.5	0.75300	0.48020	0.38821	1.76664	1.02936	0.80303

$\alpha$	Second overtone			Third overtone		
	$M_a = 3$	$M_a = 10$	$M_a = 30$	$M_a = 3$	$M_a = 10$	$M_a = 30$
-1	2.50463	1.77852	1.59824	3.55657	2.51123	2.25140
-0.5	2.54768	1.74493	1.53713	3.59392	2.44672	2.14906
0.0	2.63290	1.69280	1.43223	3.67699	2.35191	1.98756
0.3	2.72930	1.65092	1.33791	3.77286	2.27393	1.84544
0.5	2.79538	1.60990	1.24986	3.82144	2.19758	1.71171

**Table 6.** Eigenfrequencies ( $\delta_i$ ) for several modes and magnetic field strengths for  $\gamma = 5/3$  and  $\beta = 2$ .

$\alpha$	Fundamental			First overtone		
	$M_a = 3$	$M_a = 10$	$M_a = 30$	$M_a = 3$	$M_a = 10$	$M_a = 30$
-1	0.43031	0.27658	0.25635	1.45075	1.03787	0.94698
-0.5	0.47773	0.32531	0.28242	1.49626	1.05480	0.95981
0.0	0.55034	0.35176	0.30317	1.58012	1.06036	0.94929
0.3	0.62587	0.37345	0.31234	1.67378	1.07176	0.93804
0.5	0.70256	0.39530	0.31871	1.75753	1.09095	0.92967

$\alpha$	Second overtone			Third overtone		
	$M_a = 3$	$M_a = 10$	$M_a = 30$	$M_a = 3$	$M_a = 10$	$M_a = 30$
-1	2.50320	1.81950	1.68275	3.55754	2.59039	2.40284
-0.5	2.54284	1.80897	1.66530	3.59230	2.55669	2.36004
0.0	2.62573	1.78459	1.62070	3.67348	2.50237	2.28419
0.3	2.72132	1.77329	1.58450	3.76880	2.46542	2.22368
0.5	2.79310	1.77345	1.55688	3.82473	2.43991	2.17669

The loci of neutral stability in the  $\log(M_a)$ - $\alpha$  space, which separate stable and unstable regimes (for fixed  $\beta$  and  $\gamma$ ), are displayed in Fig. 4. Whereas an Alfvén number of 8 will suppress the growth of all modes of oscillation for  $\alpha > 0$  in the atomic shocks ( $\gamma = 5/3$ ,  $\beta = 2$ ), we require just  $M_a < 20$  for the equivalent molecular case.

**Table 7.** Eigenfrequencies ( $\delta_i$ ) for several modes and varying magnetic field strengths for  $\gamma = 7/5$  and  $\beta = 1$ .

$\alpha$	Fundamental			First overtone		
	$M_a = 3$	$M_a = 10$	$M_a = 30$	$M_a = 3$	$M_a = 10$	$M_a = 30$
-1	0.43865	0.27943	0.23392	1.41341	0.84427	0.69527
-0.5	0.48338	0.30069	0.25072	1.46172	0.84617	0.68237
0.0	0.55590	0.32986	0.26344	1.55387	0.85161	0.65657
0.3	0.62987	0.35788	0.27225	1.64946	0.86141	0.63397
0.5	0.69568	0.38442	0.27884	1.71604	0.86861	0.61193

$\alpha$	Second overtone			Third overtone		
	$M_a = 3$	$M_a = 10$	$M_a = 30$	$M_a = 3$	$M_a = 10$	$M_a = 30$
-1	2.43144	1.44978	1.19709	3.45026	2.04889	1.69333
-0.5	2.47796	1.42644	1.14496	3.49517	2.00664	1.61494
0.0	2.57765	1.39673	1.06321	3.60095	1.95155	1.49445
0.3	2.68125	1.37676	0.99033	3.70963	1.90977	1.38357
0.5	2.73264	1.35376	0.92053	3.74108	1.85977	1.27176

**Table 8.** Eigenfrequencies ( $\delta_i$ ) for the various modes of parameters  $\gamma = 7/5$  and  $\beta = 2$  for various magnetic fields.

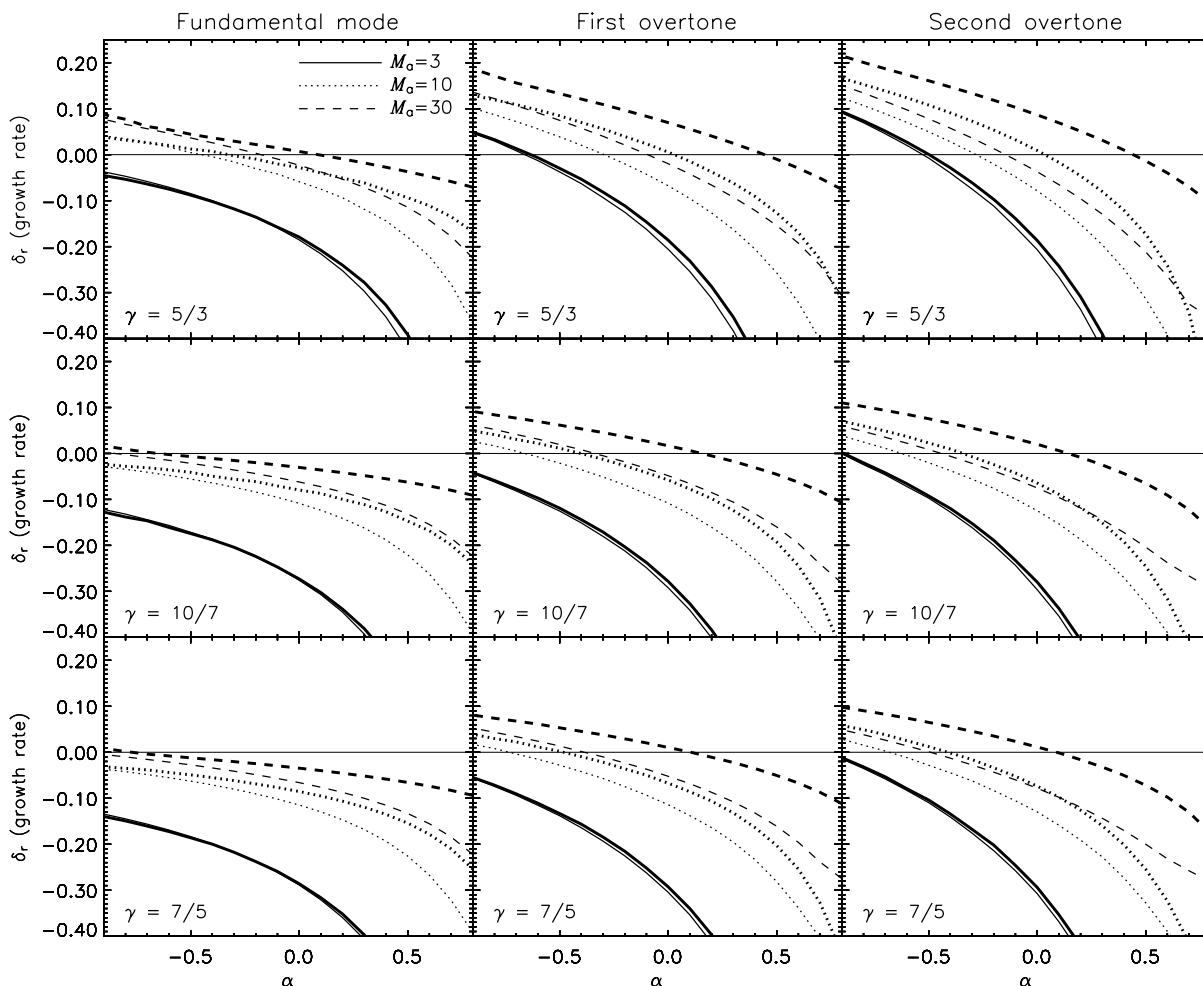
$\alpha$	Fundamental			First overtone		
	$M_a = 3$	$M_a = 10$	$M_a = 30$	$M_a = 3$	$M_a = 10$	$M_a = 30$
-1	0.42613	0.24811	0.19424	1.41061	0.84868	0.71088
-0.5	0.46608	0.26937	0.21581	1.45638	0.85532	0.71608
0.0	0.53258	0.29198	0.22668	1.54505	0.86521	0.70578
0.3	0.60136	0.31426	0.23328	1.63895	0.88205	0.69826
0.5	0.66468	0.33806	0.23891	1.70814	0.90367	0.69442

$\alpha$	Second overtone			Third overtone		
	$M_a = 3$	$M_a = 10$	$M_a = 30$	$M_a = 3$	$M_a = 10$	$M_a = 30$
-1	2.42930	1.47335	1.25896	3.44982	2.09150	1.79406
-0.5	2.47396	1.46111	1.23842	3.49352	2.06317	1.75504
0.0	2.57015	1.44656	1.20060	3.59567	2.02658	1.69333
0.3	2.67207	1.44242	1.17200	3.70268	2.00303	1.64574
0.5	2.72750	1.44027	1.15139	3.73955	1.97825	1.60978

Hence molecular shocks tend to be considerably more stable. On the other hand, the Alfvén number of 8 would be sufficient to stabilize even the first overtone for molecular shocks with  $\alpha = -0.5$ .

Given the trends in Fig. 4, it is not clear that higher-order modes possess wider instability ranges. In fact, from inspection of



**Figure 2.** A graphical summary of results for the stability: the growth/damping rates,  $\delta_r$ , plotted against  $\alpha$  for the fundamental, first and second modes (from left to right), the indicated different cases of  $\gamma$  (from top to bottom), different  $\beta$  (thick,  $\beta = 2$ ; thin,  $\beta = 1$ ), and three magnetic field strengths, indicated by the line styles shown in the top left-hand panel by the shock Alfvén numbers,  $M_a$ .

Tables 1–8, the growth rate tends to be lower for higher overtones for  $\alpha > 0.0$  especially as the magnetic field strength increases, whereas for  $\alpha < 0$ , however, there is an increasing trend in the growth rate. Here, we have investigated these trends for low- $M_a$  shocks to determine if the magnetic field will stabilize shocks entirely. As shown in Fig. 5, the growth rate continues to decrease as the mode number is increased for  $\alpha = 0.3$  and  $M_a = 1.5$ , taking an atomic shock for illustration. In contrast, the growth rate displays the opposite trend for the case with negative  $\alpha$ . In other words, the magnetic field may not provide complete stability for cooling with negative  $\alpha$ . However, the significance of high-order modes is probably highly restricted and a multidimensional analysis is necessary to determine any observational consequences.

The present analysis applies to both atomic and molecular shocks and assumes that the magnetic field is parallel to the shock front. However, in a sufficiently strong shock the molecules will dissociate immediately following the shock jump. In fact, dissociative cooling may dominate the cooling function. Given a molecular medium with Alfvén speed of  $1 \text{ km s}^{-1}$  (Crutcher 1999) and a speed limit for molecular shocks of  $40 \text{ km s}^{-1}$  at low densities (under  $\sim 10^4 \text{ cm}^{-3}$ ) and  $\sim 24 \text{ km s}^{-1}$  at high cloud densities (Smith 1994a), the maximum Alfvén number for molecular shocks with  $\gamma = 7/5$  is then in the range 24–40.

A maximum value for the magnetic field should also exist, above which ambipolar diffusion dominates the shock physics. The limit is more difficult to calculate since it depends on the ionization fraction, density and cooling function. In fact, the limitation is much stronger on the ion fraction rather than the magnetic field. In molecular clouds that are well shielded from the extreme ultraviolet, the ion fraction,  $\chi$ , is extremely low and ambipolar diffusion dominates. On the other hand, the ion fraction may reach high values near massive stars, stellar outflows or within bow shocks with high-speed apices, supplying ionizing radiation. As estimated by Smith & Brand (1990), ion fractions exceeding  $\sim 10^{-5} B_{-3}/n_6^{3/2}$  ( $\text{H}_2\text{O}$  cooling) or  $\sim 2 \times 10^{-6} B_{-3}/n_6^{1/2}$  ( $\text{H}_2$  cooling) are required to ensure a J-type shock, where  $B_{-3} = B/(10^{-3} \text{ G})$  and  $n_6 = n/(10^6 \text{ cm}^{-3})$ . Thus, the Alfvén speed must not exceed  $\sim 5 \times 10^5 n_6 \chi \text{ km s}^{-1}$  ( $\text{H}_2\text{O}$  cooling) or  $\sim 10^5 \chi \text{ km s}^{-1}$  ( $\text{H}_2$  cooling).

#### 4 CONCLUSIONS: MOLECULAR SHOCK

We have found the stable and unstable regions for radiative shocks in the  $\alpha$ ,  $\beta$  and  $\gamma$  parameter space for various magnetic field strengths and in the field  $\alpha$  parameter space for specific  $\beta$  and  $\gamma$  values.

For the fundamental mode, molecular shocks are considerably more stable than atomic shocks. For the overtones, molecular shocks

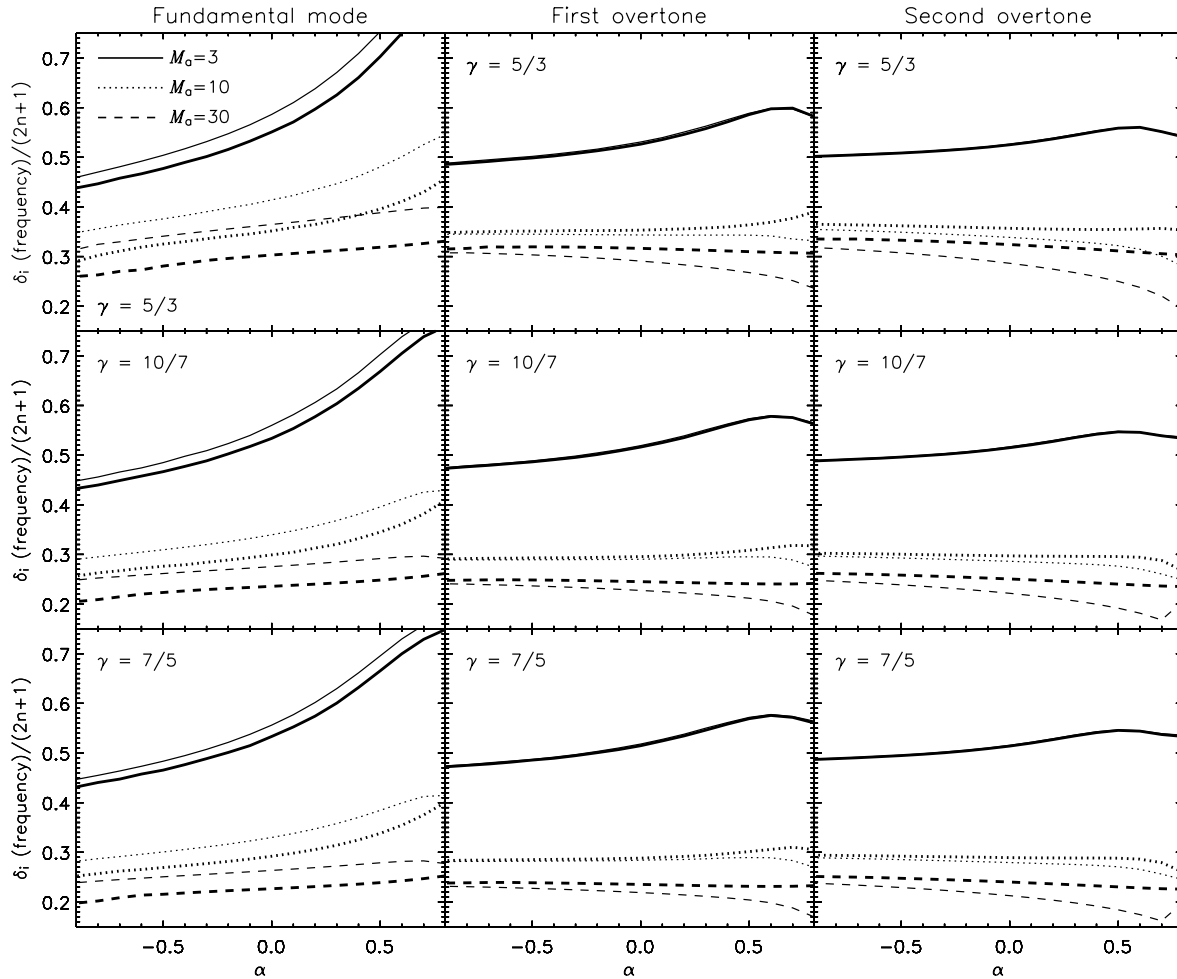


**Figure 3.** A graphical summary of results for the frequency. The frequency,  $\delta_i$ , plotted here against  $\alpha$ , has been normalized by the factor  $1/(2n + 1)$ , where  $n$  is the mode number (fundamental being  $n = 0$ ), which demonstrates that the modes resemble that of a half-open organ pipe. Displayed are results for the fundamental, first and second modes (from left to right), the indicated different cases of  $\gamma$  (from top to bottom), different  $\beta$  (thick,  $\beta = 2$ ; thin,  $\beta = 1$ ), and three magnetic field strengths, indicated by the line styles shown in the top left-hand panel by the shock Alfvén numbers,  $M_a$ .

are only moderately more stable. The magnetic field, however, has a strong stabilizing influence on all these modes, decreasing all the growth rates by similar factors (see Fig. 2).

The field strength enters the stability condition through the shock Alfvén number. All cooling functions in which the cooling increases with temperature are stable for  $M_a < 20$ . However, for  $M_a > 22$ , the first overtone can be unstable, potentially leading to oscillations with non-linear amplitudes. Hence, we need to estimate the Alfvén number for typical shocks in various environments.

Unfortunately, in molecular clouds, the Alfvén speed is a very uncertain parameter. It is even difficult to get an objective view on the magnetic field strength alone (Padoan & Nordlund 1999), although derived Alfvén speeds generally lie within the range  $0.5\text{--}5\text{ km s}^{-1}$  (Crutcher 1999). Jump shocks followed by cooling zones can arise without molecular dissociation for shock speeds as high as  $40\text{ km s}^{-1}$  at low densities but  $\sim 24\text{ km s}^{-1}$  at high cloud densities (Smith 1994a). As discussed in Section 3, a minimum ion fraction is also required to maintain a frozen-in magnetic field. Hence, a quite fast shock in a diffuse molecular cloud is the most favourable state for the appearance of oscillations.

The temperature dependence of molecular cooling functions generally correspond to values of  $\alpha$  well above zero and so indicates stable shocks. However, besides temperature and density, shock cooling may depend on the chemistry. The rate of formation of trace molecules within the cooling layer can increase the cooling rate as the temperature falls. In particular, the propagation of warming but non-ionizing shocks into cool atomic gas may show trace molecule formation and increasing cooling within a gas with  $\gamma = 5/3$ . However, because of the low shock speeds, these shocks would be stabilized if the magnetic field were transverse. Hence, it may be that oblique non-ionizing shock waves into atomic gas represent the rather restrictive conditions for shock instability within the cool components of the interstellar medium.

Although it is well known how an oblique field alters the nature of a steady shock, it is not clear how it alters the stability conditions. It should also be noted that the magnetic field may help to stabilize shocks even when the field is parallel to the shock provided the Alfvén number is less than the Mach number, a condition expected to be satisfied in molecular clouds (Smith 1993). Such an analysis, as well as multidimensional numerical simulations of radiative shocks, are still to be performed.

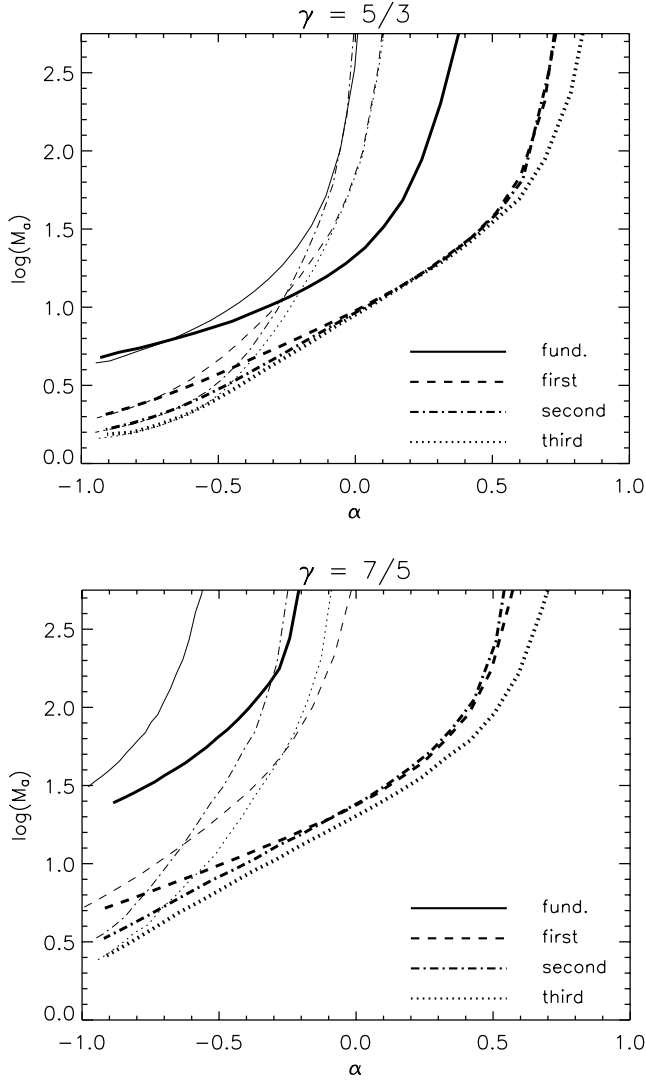


**Figure 4.** The loci of neutral stability for the indicated values of  $\gamma$ , modes and  $\beta = 2$  (thick lines) and  $\beta = 1$  (thin lines). Here  $\log(M_a)$  is plotted against  $\alpha$ . The region of instability is above the lines in all cases.

#### ACKNOWLEDGMENTS

Research at Armagh Observatory is funded by the Department of Culture, Arts and Leisure, Northern Ireland. BR is extremely grateful to Sathya Sai Baba for inspiration and also thanks Professor S. Kandaswami for encouragement and advice.

#### REFERENCES

- Chevalier R. A., Imamura J. N., 1982, *ApJ*, 261, 543  
 Crutcher R. M., 1999, *ApJ*, 520, 706  
 Imamura J. N., Aboasha A., Wolff M. T., Wood K. S., 1996, *ApJ*, 458, 327  
 Kimoto P. A., Chernoff D. F., 1997, *ApJ*, 487, 728  
 Langer S. H., Chanmugam G., Shaviv G., 1981, *ApJ*, 245, L23  
 Padoan P., Nordlund Å., 1999, *ApJ*, 526, 279  
 Ramachandran B., Smith M. D., 2005, *MNRAS*, 357, 707 (Paper 1)  
 Smith M. D., 1989, *MNRAS*, 238, 235  
 Smith M. D., 1993, *A&A*, 272, 571  
 Smith M. D., 1994a, *MNRAS*, 266, 238  
 Smith M. D., 1994b, *A&A*, 289, 256  
 Smith M. D., Brand P. W. J. L., 1990, *MNRAS*, 242, 495  
 Toth G., Draine B. T., 1993, *ApJ*, 413, 176 (TD93)

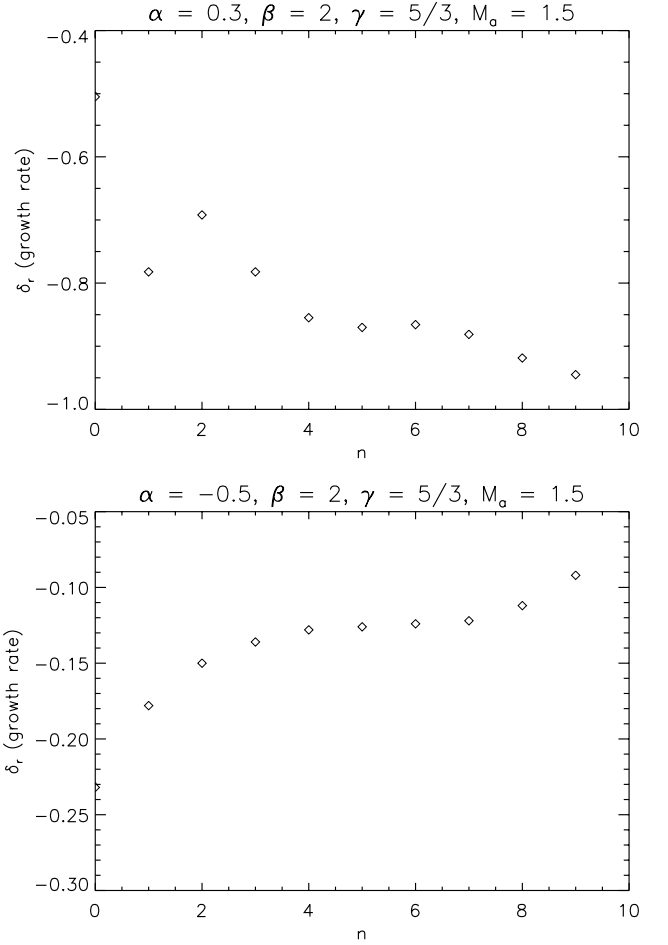


**Figure 5.** The growth rate for various overtones in the presence of a strong transverse magnetic field for the cases  $\alpha = 0.3$  (upper panel) and  $\alpha = -0.5$  (lower panel) on taking  $\beta = 2$ ,  $\gamma = 5/3$  and  $M_a = 1.5$ .

#### APPENDIX A: THE DIFFERENTIAL EQUATIONS

From equations (36), (37) and (38), we get six coupled first-order equations:

$$\begin{aligned} \frac{d\eta_r}{dw} = & \frac{\alpha\pi_r\delta^2 + (\delta_r\zeta_r + \delta_i\zeta_i) \left[ \frac{(\beta+\alpha)\theta}{w} - w(\beta-\alpha)(1+w+\theta) \right]}{(1+w+\theta - \frac{\theta}{w^2})\delta^2} \\ & + \frac{2\xi\delta^2 - 2\eta_r\delta^2 - \gamma\pi_r\delta^2 + \left[ w^2 + \frac{2(2-\gamma)\theta}{w} \right] (\zeta_r\delta_r + \zeta_i\delta_i)}{\left[ w + \gamma(w+1+\theta) + \frac{(2-\gamma)\theta}{w^2} \right] \delta^2} \\ & - \frac{d\xi}{dw} \left[ \frac{\delta_r(\eta_r + \pi_r) - \delta_i(\eta_i + \pi_i)}{w + \gamma(w+1+\theta) + \frac{(2-\gamma)\theta}{w^2}} \right] + \frac{\delta_r}{\delta^2}, \end{aligned} \quad (\text{A1})$$

$$\begin{aligned} \frac{d\eta_i}{dw} = & \frac{\alpha\pi_i\delta^2 + (\delta_r\zeta_i - \delta_i\zeta_r) \left[ \frac{(\beta+\alpha)\theta}{w} - w(\beta-\alpha)(1+w+\theta) \right]}{(1+w+\theta - \frac{\theta}{w^2})\delta^2} \\ & + \frac{-2\eta_i\delta^2 - \gamma\pi_i\delta^2 + \left[ w^2 + \frac{2(2-\gamma)\theta}{w} \right] (\zeta_i\delta_r - \zeta_r\delta_i)}{\left[ w + \gamma(w+1+\theta) + \frac{(2-\gamma)\theta}{w^2} \right] \delta^2} \\ & - \frac{d\xi}{dw} \left[ \frac{\delta_i(\eta_r + \pi_r) + \delta_r(\eta_i + \pi_i)}{w + \gamma(w+1+\theta) + \frac{(2-\gamma)\theta}{w^2}} \right] - \frac{\delta_i}{\delta^2}, \end{aligned} \quad (\text{A2})$$

$$\frac{d\pi_r}{dw} = \frac{-\xi}{w} + \frac{(\delta_r\eta_r - \delta_i\eta_i)}{w} \frac{d\xi}{dw} + \frac{\eta_r}{w} + \frac{d\eta_r}{dw} - \frac{w(\zeta_r\delta_r + \zeta_i\delta_i)}{\delta^2}, \quad (\text{A3})$$

$$\frac{d\pi_i}{dw} = \frac{(\delta_i\eta_r + \delta_r\eta_i)}{w} \frac{d\xi}{dw} + \frac{\eta_i}{w} + \frac{d\eta_i}{dw} - \frac{w(\zeta_i\delta_r - \zeta_r\delta_i)}{\delta^2}, \quad (\text{A4})$$

$$\begin{aligned} \frac{d\zeta_r}{dw} &= \frac{\xi\delta_r}{w^3} - \frac{d\xi}{dw} \frac{\zeta_r\delta_r}{w} + \frac{\delta_r}{w^2} \frac{d\eta_r}{dw} - \frac{\eta_r\delta_r}{w^3} - \frac{\delta_r(\zeta_r\delta_r + \zeta_i\delta_i)}{w\delta^2} \\ &+ \frac{d\xi}{dw} \frac{\zeta_i\delta_i}{w} - \frac{\delta_i}{w^2} \frac{d\eta_i}{dw} + \frac{\eta_i\delta_i}{w^3} + \frac{\delta_i(\zeta_i\delta_r - \zeta_r\delta_i)}{w\delta^2}, \end{aligned} \quad (\text{A5})$$

$$\begin{aligned} \frac{d\zeta_i}{dw} &= \frac{\xi\delta_i}{w^3} - \frac{d\xi}{dw} \frac{\zeta_i\delta_r}{w} + \frac{\delta_r}{w^2} \frac{d\eta_i}{dw} - \frac{\eta_i\delta_r}{w^3} - \frac{\delta_r(\zeta_i\delta_r - \zeta_r\delta_i)}{w\delta^2} \\ &- \frac{d\xi}{dw} \frac{\zeta_r\delta_i}{w} + \frac{\delta_i}{w^2} \frac{d\eta_r}{dw} - \frac{\eta_r\delta_i}{w^3} - \frac{\delta_i(\zeta_r\delta_r + \zeta_i\delta_i)}{w\delta^2}. \end{aligned} \quad (\text{A6})$$

## APPENDIX B: BOUNDARY CONDITION AT THE SHELL

Following TD93, we exploit the condition that the temperature tends to zero at the shell. This implies that the only pressure at the shell is due to the magnetic field. To extract the boundary condition, we represent the physical quantities as

$$\rho = \rho_0(x) + \rho_1(x) e^{i(ft+kx)}, \quad (\text{B1})$$

$$P = P_0(x) + P_1(x) e^{i(ft+kx)}, \quad (\text{B2})$$

$$v = v_0(x) + v_1(x) e^{i(ft+kx)}, \quad (\text{B3})$$

where  $k$  is the wavenumber, which represents the direction of the outgoing wave towards the shell, and  $f$  is the frequency. The above equations are substituted in (5) and (6) to yield

$$\frac{f}{k} = - \left( \frac{\rho_0 v_1 v_0 + P_1}{\rho_0 v_1} \right), \quad (\text{B4})$$

$$\frac{f}{k} = - \left( \frac{\rho_0 v_1 + \rho_1 v_0}{\rho_1} \right). \quad (\text{B5})$$

Equating the above expressions leads to

$$P_1 = \frac{\rho_0^2 v_1^2}{\rho_1}. \quad (\text{B6})$$

The magnetic pressure is given by

$$P = \frac{B^2}{8\pi}. \quad (\text{B7})$$

We now express the magnetic field in terms of density for example (Smith 1989) as

$$\frac{B}{B_a} = \frac{\rho}{\rho_a}, \quad (\text{B8})$$

where  $B$  and  $\rho$  are the post-shock magnetic field and density. Substituting (B2) in (B7) and defining the Alfvén velocity as  $v_a = \sqrt{B^2/(4\pi\rho)}$ , we get

$$P_1 = v_a^2 \rho_1. \quad (\text{B9})$$

Equations (B6) and (B9) yield the boundary condition at the shell as

$$P_1 = -v_a v_1 \rho_0. \quad (\text{B10})$$

The minus sign indicates the direction of the gas flow. Note that the perturbed quantities are functions of  $x$ , which itself is a function of  $\xi$  from (25). The expression (B10) can be written in terms of non-dimensional quantities as

$$\pi = -\eta \sqrt{\frac{2\theta}{-w_f^3}}. \quad (\text{B11})$$

The above quantities are evaluated at the shell boundary or equivalently at  $w = w_f$ .

This paper has been typeset from a  $\text{\TeX}/\text{\LaTeX}$  file prepared by the author.